E1B-55K mediated regulation of RNF4 STUbL promotes HAdV gene expression

Sarah Müncheberg[1,2], Ron T. Hay[3], Wing H. Ip[2], Tina Meyer[2], Christina Weiß[1], Jara Brenke[4], Sawinee Masser[1], Kamyar Hadian[4], Thomas Dobner[2] and Sabrina Schreiner[1]*

[1]Institute of Virology, Technische Universität München/Helmholtz Zentrum München, Munich, Germany

[2]Wellcome Trust Centre for Gene Regulation and Expression, College of Life Sciences, University of Dundee, Dundee, UK

[3]Heinrich Pette Institute, Leibniz Institute for Experimental Virology, Hamburg, Germany

[4]Assay Development and Screening Platform, Institute of Molecular Toxicology and Pharmacology, Helmholtz Zentrum München, Neuherberg, Germany

*Corresponding author Phone: +49 89 3187 3466

Fax: +49 89 3187 3329

Email: sabrina.schreiner@tum.de

Running title: RNF4 supports HAdV infection

Keywords: human adenovirus/HAdV/RNF4/E1B-55K/Daxx/PML-NB/SUMO/ Ubiquitin/STUbL

Abstract

HAdV E1B-55K is a multifunctional regulator of productive viral replication and oncogenic transformation in non-permissive mammalian cells. These functions depend on E1B-55K's posttranslational modification with the SUMO protein and its binding to HAdV E4orf6. Both early viral proteins recruit specific host factors to form an E3 Ubiquitin ligase complex that targets antiviral host substrates for proteasomal degradation. Recently, we reported that the PML-NB-associated factor Daxx represses efficient HAdV productive infection and is proteasomally degraded via a SUMO-E1B-55K-dependent, E4orf6-independent pathway, the details of which remained to be established.

RNF4, a cellular SUMO-targeted Ubiquitin ligase (STUbL), induces ubiquitinylation of specific SUMOylated proteins and plays an essential role during DNA repair. Here, we show that E1B-55K recruits RNF4 to the insoluble nuclear matrix fraction of the infected cell to support RNF4/Daxx association, promoting Daxx PTM, and thus inhibiting this antiviral factor. Removing RNF4 from infected cells using RNAi resulted in blocking the proper establishment of viral replication centers and significantly diminished viral gene expression. These results provide a model for how HAdV antagonize the antiviral host responses by exploiting the functional capacity of cellular STUbLs. Thus, RNF4 and its STUbL function represent a positive factor during lytic infection and a novel candidate for future therapeutic antiviral intervention strategies.

Importance

Daxx is a PML-NB-associated transcription factor, which was recently shown to repress efficient HAdV productive infection. To counteract this antiviral measurement during infection, Daxx is degraded via a novel pathway including viral E1B-55K and host proteasomes. This virus-mediated degradation is independent of the classical HAdV E3 Ubiquitin ligase complex, which is essential during viral infection to target other host antiviral substrates. To maintain productive viral life cycle, HAdV E1B-55K early viral protein inhibits the chromatin-remodeling factor Daxx in a SUMO-dependent manner. In addition viral E1B-55K protein recruits the STUbL RNF4 and sequesters it into the insoluble fraction of the infected cell. E1B-55K promotes complex formation between RNF4 and E1B-55K targeted Daxx protein, supporting Daxx posttranslational modification prior to functional inhibition. Hence, RNF4 represents a novel host factor, which is beneficial for HAdV gene expression by supporting Daxx counteraction. In this regard, RNF4 and other STUbL proteins might represent novel targets for therapeutic intervention.

Introduction

PTM (posttranslational modification) of substrate proteins with Ubiquitin or SUMO (small Ubiquitin-like modifier) has been shown to regulate a diverse number of cellular processes, including proteasomal protein degradation, transcription factor activity, nuclear/cytoplasmic shuttling and DDR (DNA damage response) (1, 2). Intriguingly, several pathogens have evolved strategies to take advantage of the cellular Ubiquitin and SUMO machinery, either by modulating essential viral proteins or restricting cellular protein functions by PTM (3).

HAdV (Human Adenoviruses) counteract cellular antiviral responses by producing the E1B-55K (early region 1B 55 kDa) protein that targets cellular proteins, such as Mre11, p53, DNA ligase IV, Tip60, Integrin α3, ATRX and SPOC1 for proteasomal degradation in cooperation with the E4orf6 (early region 4 open reading frame 6) protein. Together with a variety of host factors, such as Cullin5, Rbx1/RCO1/Hrt1, and Elongins B/C they assemble an SCF-like E3 Ubiquitin ligase complex (3, 4).

We reported previously, that the transcriptional repressor Daxx (death domain–associated protein) represents a negative regulator of HAd5 gene expression during productive infection (5-11). Daxx is mainly found in the nucleus, associated to PML-NBs (PML nuclear bodies), or at heterochromatin areas in a complex with ATRX (X-linked α-thalassaemia retardation syndrome protein) (2, 12). PML-NB association of Daxx was found to alleviate gene repression and activate apoptosis, while chromatin-bound Daxx acts in a transcriptionally repressive manner (13-15). Daxx association to either PML-NBs or chromatin depends on the status of the host cell and on the interaction of Daxx with other nuclear proteins (e.g. PML, ATRX), which

92 can be regulated by PTM. Ishov and collegues also observed that cell cycle
93 dependent phosphorylation regulates the exit of Daxx from PML-NBs prior to
94 assembly to ATRX and chromatin-associated proteins like histone deacetylases,
95 acetylated histone H4 and DEK at condensed chromatin regions (16-18).

96 We demonstrated that the functional Daxx/ATRX chromatin-remodeling complexes
97 in the nucleus of infected cells efficiently repress HAdV replication (19, 20). These
98 data provide evidence that chromatin-modulating proteins play a major role during
99 host cell intrinsic defense mechanism against HAdV. To oppose this repression, this
100 virus antagonizes ATRX protein concentrations by proteasomal degradation via the
101 E1B-55K/E4orf6 E3 Ubiquitin ligase complex during productive infection (21). In
102 addition, we also discovered that E1B-55K alone inhibits the innate antiviral
103 activities of Daxx by targeting this cellular protein for proteasomal degradation via a
104 so far unknown proteasome-dependent pathway, independent of E4orf6 (21). These
105 findings illustrate the importance of E1B-55K in processes blocking innate antiviral
106 activities.

107 The cellular RNF4 (RING-finger protein 4) protein is a member of the STUbL
108 (SUMO-targeted Ubiquitin ligases) protein family (2). STUbL proteins bind via
109 SUMO-SIM interaction on SUMO-conjugated factors and thereby promote
110 ubiquitinylation and proteasomal degradation of SUMO-modified target proteins.
111 (22). RNF4 contains four functional SIM regions in the N-terminus and a RING-
112 domain at the C-terminal region, which is responsible for dimerization and
113 activation of the ligase activity (23). Importantly, RNF4 mediates the
114 ubiquitinylation, and thus proteasomal degradation of SUMO-modified PML, the

scaffolding factor of PML-NBs (22, 24, 25) (26). Since PML-NBs are involved in virus infection, it is not surprising that RNF4 severely affects viral life cycles (22).

Here, we show that RNF4 is sequestered into the insoluble nuclear matrix fraction of the host cell during HAdV infection. This relocalization is mediated by RNF4 interaction with E1B-55K, independently of the SIM and ARM regions in the host protein. Furthermore, we provide evidence that E1B-55K connects RNF4 with the anti-HAdV transcription factor Daxx to simultaneously modulate Daxx PTM. This block of antiviral capacity is supported by the finding that HAdV gene expression is reduced in RNF4 depleted cells. Taken together, our data demonstrate that E1B-55K together with RNF4 foster Daxx PTM most presumably prior to Daxx proteasomal degradation during HAdV infection, thus RNF4 expression is favorable for viral gene expression and replication.

Material and Methods

Cell culture and generation of knock down cell lines.

H1299 (ATCC *Global Bioresource Center*, No. CRL-5803) and HEK293 cells (ECACC *European Collection of Authenticated Cell Cultures*; Sigma Aldrich, No. 85120602-1VL) were grown in Dulbecco's modified Eagle's medium supplemented with 10% fetal calf serum, 100U of penicillin, 100µg of streptomycin per ml in a 5% CO_2 atmosphere at 37°C. To generate RNF4 knock down cell lines, H1299 cells were transduced with lentiviral vectors expressing shRNA targeted to the coding strand sequence 5'-CCGGACGTATATGTGACTACCCATACTCGAGTATGGGTAGTCACATATACGT TTTTTG-3' (Sigma Aldrich, mission RNA No. NM_002938.3 - 650s21c1). Knock down cell lines were selected and maintained in medium containing puromycin (2µg/ml). All cell lines are frequently tested for mycoplasma contamination.

Plasmids and transient transfections.

HAdV-C5 proteins examined in this study were expressed from their respective complementary DNAs under the control of CMV immediate-early promoter, derived from the pcDNA3 vector (Invitrogen) to express E1B-55K and accordingly E1B-55K-mutants (27). SFB (S tag, Flag epitope tag, and streptavidin-binding peptide tag)-derived wild type-, ΔARM, ΔSIM and double mutant Δ(ARM+SIM) plasmids expressing RNF4 were kindly provided by Dr. Junjie Chen. RNF4 point mutations were introduced by site-directed mutagenesis using oligonucleotides shown in Table 1. pcDNA3 derived pUbiquitin-His plasmid was kindly provided by Prof. Ron Hay. pDaxx-HA protein was expressed from pcDNA3 derived vector under CMV

immediate-early promoter. shDaxx was targeted to the coding strand sequence 5'-GGAGTTGGATCTCTCAG AA-3` located at nt 626–643 in Daxx (28, 29). For transient transfections subconfluent cells were treated with a mixture of DNA and 25kDa linear polyethylenimine (PEI) as described recently (21).

Viruses. H5*pg*4100 served as the wild type (wt) virus (30). H5*pm*4149 carries stop codons in the E1B-55K open reading frames to prevent expression of E1B-55K (31) (32). Viruses were propagated and titrated in HEK293 cells. For this, infected cells were harvested after 48h p.i. and lysed by three times of freeze and thaw and reinfected into HEK293 cells. Virus growth was determined by immunofluorescence staining of the adenoviral DNA binding protein E2A/DBP.

Antibodies and protein analysis. Primary antibodies specific for viral proteins included E1B-55K mouse mAb 2A6 (33), E4orf6 mouse mAb RSA3 (34), L4-100K rat mAb 6B-10 (35), E2A/DBP mouse mAb B6-8 (36), E1A mouse mAb M73 (37), and HAdV-5 rabbit polyclonal serum L133 (38). Primary antibodies specific for cellular and ectopically expressed proteins included Daxx rabbit pAb 07-471 (Upstate), RNF4 mouse pAb A01 (Abnova), RNF4 mouse mAb (kindly provided by T. Urano), GAPDH Ab (sc-32233; Santa Cruz), H3 (Histon 3) Ab (1326-1; Epitomics), Mre11 rabbit pAB pNB 100-142 (Novus Biologicals, Inc.), α-Flag mouse mAb M2 (Sigma-Aldrich, Inc.), α-HA-tag rat mAb (Roche), α-Ubiquitin mouse mAb (FK2; Affinity Research), α-His-tag mouse mAb (Clontech), and ß-actin mouse mAb AC-15 (Sigma-Aldrich, Inc.). Secondary Ab conjugated to horseradish peroxidase (HRP) for

detection of proteins by immunoblotting were aα-rabbit IgG, α-mouse IgG, α-mouse light chain IgG and α-rat IgG (Jackson/Dianova). All protein extracts were prepared in RIPA lysis buffer as described recently (39). For immunoprecipitation, protein A-Sepharose beads (Sigma-Aldrich Inc.) coupled with 1µg of Ab for 1h at 4°C were used (3mg/immunprecipitation). The Ab-coupled protein A-Sepharose was added to pansorbin-Sepharose (50µl/lysate; Calbiochem) precleared extracts and rotated for 2h at 4°C. Proteins bound to the Ab-coupled protein A-Sepharose were precipitated by centrifugation, washed three times, boiled for 5min at 95°C in 2x Laemmli buffer, and analyzed by immunoblotting. Cell fractionation was performed based on a modified protocol described by Leppard et al (40), which we reported previously (41). For Ni-NTA pull down, cells were harvested 48h after treatment. 20% of cells were pelleted to determine steady-state protein concentrations as described above, whereas the remaining cells were resuspended in 5ml guanidinium hydrochloride (GuHCl) lysis buffer (0.1M Na_2HPO_4, 0.1M NaH_2PO_4, 10mM Tris/HCl pH 8.0, 20mM Imidazole and 5mM β-mercaptoethanol). Lysed cells in GuHCl were sonicated for 30s (40 pulses, output 0.6, 0.8 impulses/s) and supplemented with 25µl Ni-NTA agarose (Qiagen) prewashed with GuHCl. The samples were incubated over night at 4°C followed by centrifugation (4000rpm, 10min, 4°C). Sedimented agarose was washed once with buffer A (8M urea, 0.1M Na_2HPO_4, 0.1M NaH_2PO_4, 10mM Tris/HCl pH 8.0, 20mM imidazole and 5mM β-mercaptoethanol) and two times with buffer B (8M urea, 0.1M Na_2HPO_4, 0.1M NaH_2PO_4, 10mM Tris/HCl pH 6.3, 20mM imidazole and 5mM β -mercaptoethanol). 6His-Ubiquitin conjugates were eluted from the Ni-NTA agarose with 30µl Nickel

resin elution buffer (200mM imidazole, 5% (w/v) SDS, 150mM Tris/HCl (pH 6.7), 30% (v/v) glycerol, 720mM β-mercaptoethanol, 0.01% (w/v) bromophenol blue). After denaturation, proteins were separated by SDS-PAGE, transferred to nitrocellulose blotting membranes (0.45µm) and visualized by immunoblotting. Autoradiograms were scanned and cropped using Adobe Photoshop CS6 and Figures were prepared using Adobe Illustrator CS6 software.

Ubiquitinylation Assay. Cells transfected were treated with 10µM MG132 and 25mM NEM for 4h before harvesting to inhibit proteasome and protease function. Lysis was performed in 1% SDS lysis buffer (150mM NaCl; 25mM Hepes (pH 7.5); 0.2% NP-40; 1mM Glycerol; 10mM NaF; 8mM ß-Glycerophosphat; 1mM DTT; 300µM Sodium-vanadate; complete protease inhibitor and 1% SDS). For immunprecipitation lysates were immunoprecipitated with Daxx Ab, followed by immunblotting with α-Daxx and α-Ubiquitin Ab.

Indirect immunofluorescence. For indirect immunofluorescence H1299 cells were grown on glass coverslips in 1.5x10E5 cells per well. At different times cells were fixed in 4% paraformaldehyd (PFA) for 20min at 4°C or with ice-cold ethanol for 10min at -20°C. Subsequently cells were permeabilized in PBS with 0.5 Triton X-100 for 5min at room temperature. After 15min blocking in tris-buffered saline-BG (TBS-BG; BG is 5% (wt/vol) BSA and 5% (wt/vol) glycine) buffer coverslips were treated for 30min with the indicated primary antibody diluted in PBS, washed three times in TBS-BG. After 20min incubation with the corresponding Alexa 488 (Invitrogen)- or

Cy3 (Dianova)-conjugated secondary antibodies they were washed two times in TBS-BG and one time in PBS. The coverslips were then mounted in Glow medium (Energene) and digital images were acquired with a confocal laser scanning microscope (Nikon). Images were sampled to Nyquist and analyzed using Fiji (40).

Results

HAdV infection sequesters RNF4 STUbL into the insoluble matrix fraction of the host cell nucleus. Since host DNA damage repair (DDR) impedes viability and propagation of DNA viruses, HAdV efficiently target a multitude of host cell DDR repair regulatory factors such as Mre11 and SPOC1 in order to promote productive infection (42). RNF4 plays a critical role in the cellular response to DNA double strand breakes (DSB), prompting us to examine RNF4 protein levels in low-salt RIPA extracts from infected human cells (Fig. 1A, left panel). We observed that RNF4 levels are reproducibly reduced in soluble extracts 48h post wild type infection (H5*pg*4100). Moreover, we confirmed that Mre11 protein levels are also significantly decreased during HAdV infection. This protein is a component of the MRN repair complex and represents a classical target of the adenoviral E3 Ubiquitin ligase complex containing E1B-55K, E4orf6 and additional host determinants (5, 8, 10, 43-45). In parallel, we also observed that the PML-NB associated Daxx protein levels are decreased during HAdV infection. This is consistent with earlier findings demonstrating that SUMOylated E1B-55K binds and sequesteres Daxx into the proteasomal pathway of the cell by a mechanism still not understood in detail (8). We note that the Daxx antibody also detects a higher migrating unspecific band, which we refer to as unspecific (see Fig. 5F).

Next, we tested RNF4 levels in mutant virus infected cells, which do not express viral E1B-55K (H5*pm*4149) (Fig. 1A, right panel). We observed that without E1B-55K present, Daxx level is not reduced, and RNF4 protein level is much less reduced compared to wild type infected cells. As expected, also Mre11 is not affected in E1B-

249 55K lacking infected cells due to a non-functional E1B-55K/E4orf6 E3 Ubiquitin
250 ligase complex.

251 Simultanously, we determined RNF4 localization during HAdV wt (H5*pg*4100)
252 infection. Intriguingly, we discovered that RNF4 is still detectable, and thus not
253 degraded 48h post infection (Fig. 1B, panel f). We even found this host STUbL
254 juxtaposed to a specific E1B-55K fraction in round-shaped aggregates within non-
255 DAPI stained regions in the nucleus (Fig. 1B, panel h, i), presumably representing
256 the insoluble fraction of the infected cell. These results show that RNF4 was
257 efficiently removed from the soluble fraction during the course of HAdV infection
258 and relocalized adjacent to E1B-55K-containing aggregates in the host nucleus.

259 To verify this observation, we next performed subcellular fractionation of infected
260 cells at eight and 72h post infection, subjected these extracts to western blot and
261 analyzed with antibodies directed against RNF4 and E1B-55K. In addition, we
262 included antibodies that recognize human Histone 3 as a control for the nuclear
263 fraction (Fig. 1C). In accordance with previous observations (2), E1B-55K was found
264 in all cell fractions 72h post infection (Fig. 1C, lanes 3, 6, 7, 9). However, the larger
265 SUMOylated moieties of the viral protein were mainly observed in the insoluble
266 matrix fraction of the infected cell at 48h post infection (Fig. 1C, right panel, lane 9).
267 As expected, we detected RNF4 in cytoplasmic and soluble nuclear fractions at time
268 zero (Fig. 1C, left panel, lanes 1, 4); however the subcellular RNF4 distribution was
269 clearly perturbed during HAdV infection. By 72h post infection, this cellular STUbL
270 was completely sequestered into the insoluble matrix fraction (F5; Fig. 1C, left panel,
271 lane 6). An additional comparison with H5*pm*4149 infected cells, not expressing E1B-

272 55K, showed that relocalization of RNF4 into the nuclear matrix fraction is E1B-55K
273 dependent, as the majority of RNF4 was detected in the cytoplasm fraction 72h post
274 H5*pm*4149 infection (Fig. 1C, right panel, lanes 8 and 10) compared to wild type
275 infection (H5*pg*4100).

276 Additionally, we tested the intracellular Daxx distribution since this PML-NB
277 component and anti-HAdV factor is sequestered into the host proteasomal
278 degradation pathway during infection. Previously, we found that this process solely
279 depends on the presence of SUMO conjugated E1B-55K (46). Here, Daxx is mainly
280 detectable in the nuclear matrix fraction; however 72h post infection, Daxx showed
281 an additional band with higher molecular weight pointing to significant PTM
282 accompanied by a severe reduction in protein levels (Fig. 1C, left panel, lanes 6).

283 Hence, taken together our immunofluorescence data and fractionation assay results
284 reveal that E1B-55K localizes juxtaposed to the host STUbL RNF4 in the insoluble
285 fraction of the infected cell. In parallel, we observed reduced Daxx protein levels in
286 the same insoluble fraction during HAdV infection only when E1B-55K is expressed.

287

288 **HAdV E1B-55K protein is a novel interaction partner of the host STUbL RNF4.**
289 Given the above results, we further investigated intracellular localization of E1B-55K
290 and RNF4 in transient transfection experiments. Consistent with previous results,
291 immunofluorescence analyses in E1B-55K-transfected human cells revealed that this
292 viral protein mostly concentrates in perinuclear bodies 48h post transfection and
293 infection (2, 47). In contrast to the mostly diffuse nuclear localization 24h post
294 transfection (Fig. 2A, panel f), by 48h post transfection, RNF4 in the transiently

295 transfected cells was completely sequestered into the E1B-55K-containing aggregates
296 (Fig. 2A, panel l).

297 Since we observed recruitment of RNF4 with E1B-55K and the SUMOylated E1B-55K
298 into the insoluble matrix fraction during infection, we next tested whether E1B-55K
299 interacts with the endogenous RNF4 protein fraction in infected cells. As anticipated,
300 in wt (H5*pg*4100) infected cells, E1B-55K coimmunoprecipitated with RNF4-specific
301 antibody, revealing an interaction between both factors (Fig. 2B, lane 6). No E1B-55K
302 signal was observed in the corresponding negative controls (Fig. 2B, lane 5).
303 Agreeing with the data obtained in infected cells, we also detected RNF4 binding to
304 E1B-55K in the absence of any viral background (Fig. 2B, lane 8).

305 Next, we investigated the impact of E1B-55K SUMOylation on the protein
306 interaction with the host STUbL protein RNF4. Therefore, we coexpressed RNF4
307 with E1B-55K wt and the SUMO-deficient mutant K104R/SCS (Fig. 2C). To control
308 our findings, we also included the NES mutant of E1B-55K, which is even more
309 efficiently SUMO modified (Fig. 2A, panels g and k; 48, 49-54) than the wt protein.
310 Our results show that loss of SUMO conjugation in pE1B-55K-SCS transfected
311 human cells does not significantly impact on the binding ability between the viral
312 factor and RNF4.

313 Together these data show that HAdV induces an altered localization of the host
314 STUbL protein into specific insoluble E1B-55K-containing aggregates and that E1B-
315 55K SUMOylation does not abrogate binding of the viral factor to RNF4.

316

317 **HAdV E1B-55K interaction with RNF4 is NLS-, SIM- and ARM-independent.** To

test whether the putative RNF4 nuclear localization sequence (NLS) domain is involved in the E1B-55K-mediated relocalization of RNF4 into perinuclear aggregates, RNF4 variants with mutated NLS signals were generated. Intracellular fluorescence analyses revealed that E1B-55K-mediated relocalization of RNF4 is independent of the putative NLS in the STUbL protein, since Flag-RNF4-RTR version with mutated NLS signals was sequestered into the E1B-55K-containing aggregates in the presence of the viral protein (Fig. 3A, panel k and l). Our quantitation revealed that the E1B-55K protein was approximately 40% more efficient in relocalizing the RTR mutant of RNF4 into perinuclear body aggregates. Similarly, a mutant with a severe defect in Ubiquitin modification of the STUbL protein itself (Flag-RNF4-K5R) did not affect E1B-55K-mediated relocalization of RNF4 (Fig. 3A, panel p and q).

RNF4 contains tandem SUMO-interacting motifs (SIM), which have specific consensus sequences to interact with SUMO or SUMO-like domains of their ubiquitinylation targets (33). Besides the SIM, a conserved arginine-rich motif (ARM) acts as a novel recognition motif in RNF4 for selective target recruitment. Results obtained by intracellular fluorescence analyses showed that both factors still colocalize in the host nucleus as well as in perinuclear aggregates despite the SIM or ARM mutations in RNF4 (Fig. 3B, panel b,c and g, h and l, m). Although, quantitation analyses show no change in R-values for RNF4 colocalization with E1B-55K between wild type and SIM/ARM mutants, we observe differences in intracellular distributions of the protein complex. RNF4-SIM/E1B-55K complexes are distributed in accordance to RNF4-WT/E1B-55K complexes within perinuclear

bodies and nucleus. Interestingly, this changes when the ARM region of RNF 4 is altered, as RNF4 shows additional cytoplasmic localization in E1B-55K transfected cells (Fig. 3B, panels g and l), indicating that E1B-55K mediated relocalization into the nuclear matrix is not as efficient as with wild type RNF4 protein.

To investigate, whether the NLS, SIM, ARM or defective Ubiquitin modification mutations in RNF4 affect binding to E1B-55K, we performed additional coimmunoprecipitation studies. As anticipated, in E1B-55K-transfected human cells, E1B-55K coimmunoprecipitated with RNF4-specific antibody, confirming the interaction between both factors (Fig. 3C, lane 11-18), while no E1B-55K signal was observed in the corresponding negative controls (Fig. 3C, lane 10). We observed only a minor reduction in E1B-55K-binding to RNF4 without a functional SIM domain (Fig. 3C, lanes 12), and therefore conclude that the viral protein is not recruited via a SIM-dependent mechanism as shown for other SUMOylated targets of RNF4. The ARM region does not affect the RNF4 SIM-independent binding to E1B-55K; however reduced binding was observed with the NLS mutant Flag-RNF4-RTR (Fig. 3C, lane 18). However, Flag-RNF4-RTR still colocalized with E1B-55K, supporting the fact that reduced binding is sufficient for both proteins to localize together in perinuclear bodies and in the nucleus.

HAdV infection promotes RNF4 interaction with Daxx during infection. Next, we asked whether RNF4 binding to E1B-55K interferes with the viral factor's association with already known interaction partners such as the PML-NB-associated HAdV restriction factor Daxx. Since we had already observed intracellular localization of

Daxx within the nuclear matrix fraction together with RNF4 and E1B-55K above, we examined the binding between RNF4 and Daxx at different times post infection (Fig. 4A). We cotransfected HA-tagged Daxx and superinfected with HAdV wt virus (Fig. 4A). Our results indicate that Daxx does not show RNF4 binding in uninfected cells (Fig. 4A, lane 4). However, with ongoing increase of E1B-55K protein expression during infection (Fig. 4A, lane 1-3), we clearly detect an interaction between Daxx and RNF4 (Fig. 4A, lane 6). This supports the notion that HAdV infection and the presence of E1B-55K promotes binding between RNF4 and Daxx.

E1B-55K promotes RNF4 dependent Daxx modification with Ubiquitin moieties. Since our results imply that E1B-55K connects Daxx and the SUMO-dependent Ubiquitin ligase RNF4 during infection, we tested whether Daxx PTM and protein stability are also affected. First, cells were transfected with different combinations of Daxx, E1B-55K and RNF4 expression plasmids. Under proteasome inhibition, immunoprecipitation of Daxx showed significant Daxx modification exclusively when both proteins, E1B-55K and RNF4, are present (Fig. 4B, lane 20). These experiments substantiate the possibility that SUMOylated E1B-55K recruits Daxx and connects it to RNF4 to promote Daxx PTM and most presumably proteasomal degradation of this anti-HAdV transcription factor.

To further investigate this novel virus/host crosstalk, we transfected cells with Ubiquitin-His expression constructs and different combinations of Daxx, E1B-55K and RNF4 plasmids. Cells were not treated with proteasome inhibitors prior to harvesting and lysate preparation. Ni-NTA purification of Ubiquitin-His conjugates

revealed that the fraction of modified Daxx protein was already reduced by proteasomal degradation when E1B-55K and RNF4 were present (Fig. 4C, lane 12). We also observe that E1B-55K alone reduced the Daxx signal (Fig. 4C, lane 11) compared to Daxx levels in RNF4 expressing cells (Fig. 4C, lane 10). Intriguingly, in cells coexpressing RNF4 together with E1B-55K-SCS, the SUMOylation deficient variant of the viral protein (Fig. 4C, lane 14), we observed no change in immunoprecipitated Daxx protein fraction. This is consistent with earlier results showing that E1B-55K-SCS does not promote Daxx degradation (2, 11, 47).

RNF4 fosters E1B-55K-mediated Daxx inhibition hence enhancing HAdV gene expression. Daxx is involved in transcriptional regulation and cellular intrinsic antiviral resistance against HAdV, as confirmed by earlier results where knock-down of Daxx using RNAi techniques significantly increased adenoviral replication, including enhanced viral mRNA synthesis and viral protein expression (55-57). However, early protein E1B-55K counteracts this Daxx restriction imposed upon HAdV growth by binding and degrading Daxx through a proteasome-dependent pathway. To investigate whether RNF4 promotes this E1B-55K-mediated inhibition of Daxx' antiviral capacity, experiments were performed in human cells expressing shRNAs depleting RNF4. Reduced RNF4 RNA expression and protein sythesis was confirmed by real-time PCR analysis (Fig. 5A) and immunoblots (Fig. 5B). Reduction of RNF4 expression did not affect cell proliferation within the timeframe of six days post infection (Fig. 5C). To see the effect of RNF4 depletion on the virus life cycle, we assessed viral mRNA synthesis (Fig. 5D). HAdV transcription is promoted by RNF4

expression in infected cells, since viral early E1A mRNA production was lower in RNF4 depleted cells than in control cells (Fig. 5D, left panel). Similar results were obtained for Hexon mRNA expression, suggesting either a positive impact of the host STUbL on early gene products, or direct activation of the viral promoter (Fig. 5D, right panel). To substantiate our results, data from the replication assays suggest that RNF4 expression also supports virus progeny production, since less virus particles were synthesized in the RNF4-depleted cell culture system after 48 and 72h post infection (Fig. 5E). Interestingly, steady-state concentrations of Daxx protein levels were more efficiently reduced in infected cells expressing RNF4 compared to shRNF4 cells. Our quantification shows that 48h post infection a 3.3-fold difference in Daxx protein levels was observed, which increases up to 40-fold after 72h. These data support the idea that RNF4 contributes to proteasomal Daxx degradation (Fig. 5F, upper panel left). As the Daxx antibody detects various proteins bands, we additionally tested protein signal in cells stably depleted for Daxx expression. These data show that the antibody detects also an additional signal, which is not Daxx specific (Fig. 5F, lower panel, black asteriks). In sum, these observations substantiate our data showing a delayed Daxx reduction in shRNF4 cells (Fig. 5F, upper panel). Taken together, these results indicate that Daxx-mediated negative regulation of HAdV replication is counteracted by E1B-55K together with the host STUbL RNF4. Earlier, we reported that HAdV virus progeny production was promoted by loss of Daxx expression in Daxx depleted cells (21). To further clarify, whether RNF4 increases HAdV virus yield by Daxx inhibition, we transiently coexpressed shDaxx constructs in RNF depleted stable cell lines. We reproduced findings showing that

shDaxx expression enhances virus yield almost two fold (Fig. 5G, lane 2) compared to parental cells (Fig. 5G, lane 1). As seen above, stable depletion of RNF4 reduced efficient virus production (Fig. 5G, lane 3). However, this was restored, when simultanously the shDaxx plasmid was expressed (Fig. 5G, lane 4).

During infection it was shown that PML-NBs are relocalized by viral early proteins into track-like structures, juxtaposed to adenoviral replication centers. The question was whether such viral replication centers and PML-NBs are affected in cells depleted for RNF4. Intracellular immunofluorescence analysis revealed no significant difference in PML track formation in the absence of the host STUbL protein (Fig. 6A, panels h, j, k and l). However, detection of the viral marker protein E2A/DBP (red) intriguingly showed that compared with control cells expressing the scrambled shRNA (Fig. 6A, panels c, e and f), replication centers are not properly established in cells lacking RNF4 (Fig. 6A, panels i, k and l). Quantitative analysis showed a more diffuse staining of E2A/DBP within RNF4 depleted cells, whereas in parental cells E2A/DBP staining in replication centers were properly established (Fig. 6A, graph).

Discussion

Here, we provide evidence that the cellular STUbL RNF4 aids HAdV E1B-55K-dependent Daxx restriction during adenoviral infection. Thus, RNF4 is a novel host factor that significantly promotes HAdV infection by helping to mitigate the Daxx-mediated antiviral host response. We demonstrate that expression of viral E1B-55K promotes relocalization of RNF4 into the nuclear matrix fraction of the cell. These data supports our hypothesis that the host STUbL protein encounters Daxx to inhibit antiviral functions of this transcription factor.

SUMO conjugation of target substrates is a crucial signaling event that regulates diverse processes in the mammalian cell, such as stress response, chromosome segregation, DNA-damage response and meiosis (21). Viruses have also evolved pathways to benefit from these PTM in order to create an efficient replication milieu in the host cell (58). In both scenarios recognition of SUMOylated proteins is mostly mediated through SIMs present on effector proteins (4). The discovery of STUbLs directly links the SUMOylation process to ubiquitinylation, and thus degradation pathways. Through tandem SIMs, STUbLs recognize poly-SUMOylated proteins and target them for Lys48-linked polyubiquitinylation and degradation through their E3 Ubiquitin ligase activities. So far, only two cellular STUbLs have been identified in mammalian cells, such as RNF111/Arkadia (59) and RNF4/SNURF (60). RNF4 is a dimeric STUbL with four functional SIMs in the protein that recognize poly-SUMOylated substrates. The RING domain at the C-terminal part acts together with the SIM domains to facilitate ubiquitinylation of substrates already modified with poly-SUMO chains (61).

HAdV have acquired mechanisms that modulate SUMO- and Ubiquitin-mediated regulatory cascades leading to efficient viral propagation (61, 62). During the course of productive infection, HAdV gene products manipulate destruction pathways to prevent viral clearance or cell death prior to viral genome amplification and release of progeny. We recently demonstrated that chromatin formation by cellular SWI/SNF chromatin-remodeling, involving Daxx/ATRX-dependent processes, plays a key role in HAdV transcriptional regulation and virus-mediated transformation (3, 4). Daxx and ATRX are SUMO substrates in the cell and transiently found associated with PML nuclear bodies, large multiprotein complexes representing SUMOylation hotspots in the host-cell nucleus. Our recent reports demonstrate the importance of Daxx/ATRX chromatin-remodeling activities for efficient HAdV gene expression; we showed evidence that HAdV promoters are affected by Daxx/ATRX recruitment, leading to a significant block in viral gene expression and progeny production (2, 21, 47).

Early viral gene derepression mediated by incoming capsid protein VI (2, 21, 47) prior to E1B-55K/E4orf6-dependent restriction of Daxx/ATRX functional complexes is necessary for adenoviruses to evade antiviral host cell measures evolved to repress viral gene expression (summarized in Fig. 6B). In detail, based on our reported data, HAdV-mediated protein degradation apparently discriminates between classical E1B-55K/E4orf6-dependent (ATRX) pathways and a novel E1B-55K-dependent (Daxx) degradation route. However, it is still unclear how Daxx degradation works mechanistically, and whether this is a kinetic process due to the expression pattern or PTM of the viral protein E1B-55K itself early during HAdV infection.

RNF4 controls protein stability by ubiquitinylation of target substrates, such as PML or the oncogenic fusion protein PML-RAR (1, 63). Thus, the PML-associated factor Daxx, which interacts with the viral E1B-55K protein, might represent a novel STUbL substrate. RNF4 relies on its SIM domains to selectively bind poly-SUMO chains over monomer SUMO. For instance, only poly-SUMOylated PML proteins are recognized by RNF4 (61, 64). Here, we observe that neither RNF4 SIMs nor the ARM region is essential for the cellular STUbL to bind to E1B-55K. Perhaps substrate SUMOylation provides additional binding sites that facilitate protein ubiquitinylation and degradation by the RING domain of RNF4 protein.

Besides the mammalian STUbLs RNF4 and RNF111 (Arkadia), additional viral STUbLs such as VZV ORF61, KSHV K-Rta and HSV ICP0 (64) have been described so far. ICP0 functions as a STUbL that preferentially ubiquitinylates poly-SUMOylated PML during HSV infection as a mechanism to inhibit the antiviral activities of PML. Notably, ICP0 represents the first precise viral ortholog of the host STUbL RNF4 to target cellular proteins such as PML and associated factors (65-67).

Although it lacks the canonical RING domain, work by Bridges and coworkers suggest that the adenoviral E4orf3 might possess STUbL-like functions or recruit cellular STUbLs to regulate cellular protein stability by SUMO-mediated, Ubiquitin-dependent degradation (68). . Also HTLV-1 oncoprotein Tax is a substrate for RNF4. Upon RNF4-dependent ubiquitinylation, Tax is relocalized into the cytoplasm to activate the NF-kB pathway by direct interaction between Tax and NEMO (69). These findings provide important new insights into STUbL-mediated pathways that regulate the subcellular localization and functional dynamics of viral oncogenes .

In addition, RNF4 blocks EBV infection by ubiquitinylation of the transcription factor Rta, which is required to activate the transcription of EBV lytic genes. Upon ubiquitinylation, Rta is degraded and subsequently EBV lytic replication and virion production is inhibited (70). Here, we find that RNF4 is a positive regulator of HAdV lytic infection, since together with E1B-55K it supports Daxx inhibition.

Chromatin-modifying complexes containing Daxx have also been implicated in human cancer development. Evidence is growing for a correlation between chromatin-modifiers and tumor suppression, especially demonstrated for SWI/SNF complexes, which comprise several subunits displaying tumor suppressor activity. Functional disruption of SWI/SNF complexes may induce a state of epigenetic instability, resulting in altered chromatin structure that affects gene expression, and interferes with differentiation processes. These epigenetic changes may be closely linked to genomic instability, and predispose to oncogenic transformation (71). Indeed, we recently reported that efficient adenoviral transformation requires E1B-55K-mediated degradation of Daxx (47). In accordance with our current study, we envisage that RNF4 could contribute to cell transformation by modulating Daxx-dependent pathways in cooperation with E1B-55K, and consequently through disrupting SWI/SNF chromatin-remodeling functions. This is a particularly interesting concept given the oncogenic capabilities of certain STUbLs, which have shown to cooperate with either Daxx or associated determinants.

Further elucidating the crosstalk between the cellular and viral regulators discussed above will help us better understand the role of chromatin-remodeling in HAdV transcriptional regulation and adenoviral transformation of primary cells. Moreover,

543 further investigation of STUbLs during virus infection will help to identify novel
544 therapeutic approaches to modern antiviral therapy and inhibitor development.

545

Acknowledgment

We thank Takeshi Urano and Junjien Cheng for kindly providing reagents, Rudolph Reimer for his support with microscopic analyses and greatly appreciate the critical comments and scientific discussion from Nicole Fischer.

SM and SS were supported by the *Else Kröner-Fresenius-Stiftung*. Part of this work was supported by the *Deutsche Forschungsgemeinschaft DFG (SFB TRR179)*, *Deutsche Krebshilfe e.V.*, *Dräger Stiftung e. V*. and the *Manchot Stiftung*. The Heinrich Pette Institute, Leibniz Institute for Experimental Virology is supported by the *Freie und Hansestadt Hamburg* and the *Bundesministerium für Gesundheit* (BMG).

References

1. **Schreiner S, Martinez R, Groitl P, Rayne F, Vaillant R, Wimmer P, Bossis G, Sternsdorf T, Ruszsics Z, Dobner T, Wodrich H.** 2012. Transcriptional activation of the adenoviral genome is mediated by capsid protein. PLoS Pathog **8:**e1002549.
2. **Schreiner S, Wimmer P, Sirma H, Everett RD, Blanchette P, Groitl P, Dobner T.** 2010. Proteasome-dependent degradation of Daxx by the viral E1B-55K protein in human adenovirus-infected cells. J Virol **84:**7029-7038.
3. **Wimmer P, Schreiner S, Dobner T.** 2012. Human pathogens and the host cell SUMOylation system. J Virol **86:**642-654.
4. **Wimmer P, Schreiner S.** 2015. Viral Mimicry to Usurp Ubiquitin and SUMO Host Pathways. Viruses **7:**4854-4872.
5. **Baker A, Rohleder KJ, Hanakahi LA, Ketner G.** 2007. Adenovirus E4 34k and E1b 55k oncoproteins target host DNA ligase IV for proteasomal degradation. J Virol **81:**7034-7040.
6. **Dallaire F, Blanchette P, Groitl P, Dobner T, Branton PE.** 2009. Identification of integrin alpha3 as a new substrate of the adenovirus E4orf6/E1B 55-kilodalton E3 ubiquitin ligase complex. J Virol **83:**5329-5338.
7. **Querido E, Blanchette P, Yan Q, Kamura T, Morrison M, Boivin D, Kaelin WG, Conaway RC, Conaway JW, Branton PE.** 2001. Degradation of p53 by adenovirus E4orf6 and E1B55K proteins occurs via a novel mechanism involving a Cullin-containing complex. Genes Dev **15:**3104-3117.
8. **Stracker TH, Carson CT, Weitzman MD.** 2002. Adenovirus oncoproteins inactivate the Mre11 Rad50 NBS1 DNA repair complex. Nature **418:**348-352.
9. **Schreiner S, Wimmer P, Sirma H, Everett RD, Blanchette P, Groitl P, Dobner T.** 2010. Proteasome-dependent degradation of Daxx by the viral E1B-55K protein in human adenovirus-infected cells. Journal of virology **84:**7029-7038.
10. **Schreiner S, Kinkley S, Bürck C, Mund A, Wimmer P, Schubert T, Groitl P, Will H, Dobner T.** 2013. SPOC1-mediated antiviral host cell response is antagonized early in Human Adenovirus type 5 infection. PLoS Pathog **9:**e1003775.
11. **Schreiner S, Wimmer P, Dobner T.** 2012. Adenovirus degradation of cellular proteins. Future Microbiol **7(2):** 211-225.
12. **Ullman AJ, Hearing P.** 2008. Cellular proteins PML and Daxx mediate an innate antiviral defense antagonized by the adenovirus E4 ORF3 protein. J Virol **82:**7325-7335.
13. **Torii S, Egan DA, Evans RA, Reed JC.** 1999. Human Daxx regulates Fas-induced apoptosis from nuclear PML oncogenic domains (PODs). EMBO J **18:**6037-6049.
14. **Ishov AM, Sotnikov AG, Negorev D, Vladimirova OV, Neff N, Kamitani T, Yeh ET, Strauss JF, 3rd, Maul GG.** 1999. PML is critical for ND10 formation and recruits the PML-interacting protein daxx to this nuclear structure when modified by SUMO-1. J Cell Biol **147:**221-234.

15. **Dellaire G, Bazett-Jones DP.** 2004. PML nuclear bodies: dynamic sensors of DNA damage and cellular stress. Bioessays **26:**963-977.
16. **Xu ZX, Zhao RX, Ding T, Tran TT, Zhang W, Pandolfi PP, Chang KS.** 2004. Promyelocytic leukemia protein 4 induces apoptosis by inhibition of survivin expression. J Biol Chem **279:**1838-1844.
17. **Takahashi Y, Lallemand-Breitenbach V, Zhu J, de The H.** 2004. PML nuclear bodies and apoptosis. Oncogene **23:**2819-2824.
18. **Gostissa M, Morelli M, Mantovani F, Guida E, Piazza S, Collavin L, Brancolini C, Schneider C, Del Sal G.** 2004. The transcriptional repressor hDaxx potentiates p53-dependent apoptosis. J Biol Chem **279:**48013-48023.
19. **Ishov AM, Vladimirova OV, Maul GG.** 2004. Heterochromatin and ND10 are cell-cycle regulated and phosphorylation-dependent alternate nuclear sites of the transcription repressor Daxx and SWI/SNF protein ATRX. J Cell Sci **117:**3807-3820.
20. **Hollenbach AD, McPherson CJ, Mientjes EJ, Iyengar R, Grosveld G.** 2002. Daxx and histone deacetylase II associate with chromatin through an interaction with core histones and the chromatin-associated protein Dek. J Cell Sci **115:**3319-3330.
21. **Schreiner S, Bürck C, Glass M, Groitl P, Wimmer P, Kinkley S, Mund A, Everett RD, Dobner T.** 2013. Control of Human Adenovirus type 5 (Ad5) gene expression by cellular Daxx/ATRX chromatin-associated complexes. Nucleic Acids Res **41:**3532-3550.
22. **Tatham MH, Geoffroy MC, Shen L, Plechanovova A, Hattersley N, Jaffray EG, Palvimo JJ, Hay RT.** 2008. RNF4 is a poly-SUMO-specific E3 ubiquitin ligase required for arsenic-induced PML degradation. Nature cell biology **10:**538-546.
23. **Perry JJ, Tainer JA, Boddy MN.** 2008. A SIM-ultaneous role for SUMO and ubiquitin. Trends Biochem Sci **33:**201-208.
24. **Galanty YB, Rimma. Coates, Julia. Jackson, Stephen P.** 2012. RNF4, a SUMO-targeted ubiquitin E3 ligase, promotes DNA double-strand break repair. Genes & development **26:**1179-1195.
25. **Xu Y, Plechanovova A, Simpson P, Marchant J, Leidecker O, Kraatz S, Hay RT, Matthews SJ.** 2014. Structural insight into SUMO chain recognition and manipulation by the ubiquitin ligase RNF4. Nat Commun **5:**4217.
26. **Percherancier Y, Germain-Desprez D, Galisson F, Mascle XH, Dianoux L, Estephan P, Chelbi-Alix MK, Aubry M.** 2009. Role of SUMO in RNF4-mediated promyelocytic leukemia protein (PML) degradation: sumoylation of PML and phospho-switch control of its SUMO binding domain dissected in living cells. The Journal of biological chemistry **284:**16595-16608.
27. **Tatham MH, Rodriguez MS, Xirodimas DP, Hay RT.** 2009. Detection of protein SUMOylation in vivo. Nat Protoc **4:**1363-1371.
28. **Endter C, Kzhyshkowska J, Stauber R, Dobner T.** 2001. SUMO-1 modification is required for transformation by adenovirus type 5 early region 1B 55-kDa oncoprotein. Proc Natl Acad Sci USA **98:**11312-11317.
29. **Endter C, Hartl B, Spruss T, Hauber J, Dobner T.** 2005. Blockage of CRM1-dependent nuclear export of the adenovirus type 5 early region 1B 55-kDa

protein augments oncogenic transformation of primary rat cells. Oncogene **24:**55-64.

30. **Wimmer P, Berscheminski J, Blanchette P, Groitl P, Branton PE, Hay RT, Dobner T, Schreiner S.** 2015. PML isoforms IV and V contribute to adenovirus-mediated oncogenic transformation by functionally inhibiting the tumor-suppressor p53. Oncogene doi:10.1038/onc.2015.63.
31. **Groitl P, Dobner T.** 2007. Construction of adenovirus type 5 early region 1 and 4 virus mutants. Methods Mol Med **130:**29-39.
32. **Blanchette P, Kindsmuller K, Groitl P, Dallaire F, Speiseder T, Branton PE, Dobner T.** 2008. Control of mRNA export by adenovirus E4orf6 and E1B55K proteins during productive infection requires E4orf6 ubiquitin ligase activity. J Virol **82:**2642-2651.
33. **Kindsmuller K, Groitl P, Hartl B, Blanchette P, Hauber J, Dobner T.** 2007. Intranuclear targeting and nuclear export of the adenovirus E1B-55K protein are regulated by SUMO1 conjugation. Proc Natl Acad Sci U S A **104:**6684-6689.
34. **Sarnow P, Hearing P, Anderson CW, Reich N, Levine AJ.** 1982. Identification and characterization of an immunologically conserved adenovirus early region 11,000 Mr protein and its association with the nuclear matrix. J Mol Biol **162:**565-583.
35. **Marton MJ, Baim SB, Ornelles DA, Shenk T.** 1990. The adenovirus E4 17-kilodalton protein complexes with the cellular transcription factor E2F, altering its DNA-binding properties and stimulating E1A-independent accumulation of E2 mRNA. J Virol **64:**2345-2359.
36. **Kzhyshkowska J, Kremmer E, Hofmann M, Wolf H, Dobner T.** 2004. Protein arginine methylation during lytic adenovirus infection. Biochem J **383:**259-265.
37. **Reich NC, Sarnow P, Duprey E, Levine AJ.** 1983. Monoclonal antibodies which recognize native and denatured forms of the adenovirus DNA-binding protein. Virology **128:**480-484.
38. **Harlow E, Franza BR, Jr., Schley C.** 1985. Monoclonal antibodies specific for adenovirus early region 1A proteins: extensive heterogeneity in early region 1A products. J Virol **55:**533-546.
39. **Kindsmüller K, Groitl P, Härtl B, Blanchette P, Hauber J, Dobner T.** 2007. Intranuclear targeting and nuclear export of the adenovirus E1B-55K protein are regulated by SUMO1 conjugation. Proc Natl Acad Sci USA **104:**6684-6689.
40. **Wimmer P, Schreiner S, Everett RD, Sirma H, Groitl P, Dobner T.** 2010. SUMO modification of E1B-55K oncoprotein regulates isoform-specific binding to the tumour suppressor protein PML. Oncogene **29:**5511-5522.
41. **Leppard KN, Shenk T.** 1989. The adenovirus E1B 55 kd protein influences mRNA transport via an intranuclear effect on RNA metabolism. EMBO J **8:**2329-2336.
42. **Schindelin J, Arganda-Carreras I, Frise E, Kaynig V, Longair M, Pietzsch T, Preibisch S, Rueden C, Saalfeld S, Schmid B, Tinevez JY, White DJ, Hartenstein V, Eliceiri K, Tomancak P, Cardona A.** 2012. Fiji: an open-source platform for biological-image analysis. Nat Methods **9:**676-682.
43. **Querido E, Blanchette P, Yan Q, Kamura T, Morrison M, Boivin D, Kaelin WG, Conaway RC, Conaway JW, Branton PE.** 2001. Degradation of p53 by

694 adenovirus E4orf6 and E1B55K proteins occurs via a novel mechanism
695 involving a Cullin-containing complex. Genes Dev **15:**3104-3117.
696 44. **Orazio NI, Naeger CM, Karlseder J, Weitzman MD.** 2011. The adenovirus
697 E1b55K/E4orf6 complex induces degradation of the Bloom helicase during
698 infection. J Virol **85:**1887-1892.
699 45. **Gupta A, Jha S, Engel DA, Ornelles DA, Dutta A.** 2013. Tip60 degradation
700 by adenovirus relieves transcriptional repression of viral transcriptional
701 activator EIA. Oncogene **32:**5017-5025.
702 46. **Endter C, Hartl B, Spruss T, Hauber J, Dobner T.** 2005. Blockage of CRM1-
703 dependent nuclear export of the adenovirus type 5 early region 1B 55-kDa
704 protein augments oncogenic transformation of primary rat cells. Oncogene
705 **24:**55-64.
706 47. **Schreiner S, Wimmer P, Groitl P, Chen SY, Blanchette P, Branton PE,**
707 **Dobner T.** 2011. Adenovirus Type 5 Early Region 1B 55K Oncoprotein-
708 Dependent Degradation of Cellular Factor Daxx Is Required for Efficient
709 Transformation of Primary Rodent Cells. J Virol **85:**8752-8765.
710 48. **Zantema A, Fransen JA, Davis OA, Ramaekers FC, Vooijs GP, DeLeys B,**
711 **van der Eb AJ.** 1985. Localization of the E1B proteins of adenovirus 5 in
712 transformed cells, as revealed by interaction with monoclonal antibodies.
713 Virology **142:**44-58.
714 49. **Zantema A, Schrier PI, Davis OA, van Laar T, Vaessen RT, van der Eb AJ.**
715 1985. Adenovirus serotype determines association and localization of the
716 large E1B tumor antigen with cellular tumor antigen p53 in transformed cells.
717 Mol Cell Biol **5:**3084-3091.
718 50. **Goodrum FD, Shenk T, Ornelles DA.** 1996. Adenovirus early region 4 34-
719 kilodalton protein directs the nuclear localization of the early region 1B 55-
720 kilodalton protein in primate cells. J Virol **70:**6323-6335.
721 51. **König C, Roth J, Dobbelstein M.** 1999. Adenovirus type 5 E4orf3 protein
722 relieves p53 inhibition by E1B-55-kilodalton protein. J Virol **73:**2253-2262.
723 52. **Krätzer F, Rosorius O, Heger P, Hirschmann N, Dobner T, Hauber J,**
724 **Stauber RH.** 2000. The adenovirus type 5 E1B-55k oncoprotein is a highly
725 active shuttle protein and shuttling is independent of E4orf6, p53 and Mdm2.
726 Oncogene **19:**850-857.
727 53. **Wienzek S, Roth J, Dobbelstein M.** 2000. E1B 55-kilodalton oncoproteins of
728 adenovirus types 5 and 12 inactivate and relocalize p53, but not p51 or p73,
729 and cooperate with E4orf6 proteins to destabilize p53. J Virol **74:**193-202.
730 54. **Blanchette P, Wimmer P, Dallaire F, Cheng CY, Branton PE.** 2013.
731 Aggresome Formation by the Adenoviral Protein E1B55K Is Not Conserved
732 among Adenovirus Species and Is Not Required for Efficient Degradation of
733 Nuclear Substrates. J Virol **87:**4872-4881.
734 55. **Pennella MA, Liu Y, Woo JL, Kim CA, Berk AJ.** 2010. Adenovirus E1B 55-
735 kilodalton protein is a p53-SUMO1 E3 ligase that represses p53 and stimulates
736 its nuclear export through interactions with promyelocytic leukemia nuclear
737 bodies. Journal of virology **84:**12210-12225.
738 56. **Muller S, Dobner T.** 2008. The adenovirus E1B-55K oncoprotein induces
739 SUMO modification of p53. Cell Cycle **7:**754-758.

57. **Wimmer P, Berscheminski J, Blanchette P, Groitl P, Branton PE, Hay RT, Dobner T, Schreiner S.** 2015. PML isoforms IV and V contribute to adenovirus-mediated oncogenic transformation by functional inhibition of the tumor suppressor p53. in revision.
58. **Hay RT.** 2013. Decoding the SUMO signal. Biochem Soc Trans **41:**463-473.
59. **Song J, Durrin LK, Wilkinson TA, Krontiris TG, Chen Y.** 2004. Identification of a SUMO-binding motif that recognizes SUMO-modified proteins. Proc Natl Acad Sci U S A **101:**14373-14378.
60. **Poulsen SL, Hansen RK, Wagner SA, van Cuijk L, van Belle GJ, Streicher W, Wikstrom M, Choudhary C, Houtsmuller AB, Marteijn JA, Bekker-Jensen S, Mailand N.** 2013. RNF111/Arkadia is a SUMO-targeted ubiquitin ligase that facilitates the DNA damage response. J Cell Biol **201:**797-807.
61. **Tatham MH, Geoffroy MC, Shen L, Plechanovova A, Hattersley N, Jaffray EG, Palvimo JJ, Hay RT.** 2008. RNF4 is a poly-SUMO-specific E3 ubiquitin ligase required for arsenic-induced PML degradation. Nat Cell Biol **10:**538-546.
62. **Plechanovova A, Jaffray EG, Tatham MH, Naismith JH, Hay RT.** 2012. Structure of a RING E3 ligase and ubiquitin-loaded E2 primed for catalysis. Nature **489:**115-120.
63. **Schreiner S, Wodrich H.** 2013. Virion factors targeting Daxx to overcome intrinsic immunity. J Virol **87:**10412-10422.
64. **Lallemand-Breitenbach V, Jeanne M, Benhenda S, Nasr R, Lei M, Peres L, Zhou J, Zhu J, Raught B, de The H.** 2008. Arsenic degrades PML or PML-RARalpha through a SUMO-triggered RNF4/ubiquitin-mediated pathway. Nat Cell Biol **10:**547-555.
65. **Sriramachandran AM, Dohmen RJ.** 2014. SUMO-targeted ubiquitin ligases. Biochim Biophys Acta **1843:**75-85.
66. **Izumiya Y, Kobayashi K, Kim KY, Pochampalli M, Izumiya C, Shevchenko B, Wang DH, Huerta SB, Martinez A, Campbell M, Kung HJ.** 2013. Kaposi's Sarcoma-Associated Herpesvirus K-Rta Exhibits SUMO-Targeting Ubiquitin Ligase (STUbL) Like Activity and Is Essential for Viral Reactivation. PLoS pathogens **9:**e1003506.
67. **Boutell C, Cuchet-Lourenco D, Vanni E, Orr A, Glass M, McFarlane S, Everett RD.** 2011. A viral ubiquitin ligase has substrate preferential SUMO targeted ubiquitin ligase activity that counteracts intrinsic antiviral defence. PLoS Pathog **7:**e1002245.
68. **Bridges RG, Sohn SY, Wright J, Leppard KN, Hearing P.** 2016. The Adenovirus E4-ORF3 Protein Stimulates SUMOylation of General Transcription Factor TFII-I to Direct Proteasomal Degradation. MBio **7:**e02184-02115.
69. **Fryrear KAG, Xin. Kerscher, Oliver. Semmes, O. John.** 2012. The Sumo-targeted ubiquitin ligase RNF4 regulates the localization and function of the HTLV-1 oncoprotein Tax. Blood **119:**1173-1181.
70. **Yang YC, Yoshikai Y, Hsu SW, Saitoh H, Chang LK.** 2013. Role of RNF4 in the ubiquitination of Rta of Epstein-Barr virus. J Biol Chem **288:**12866-12879.
71. **Wilson BG, Roberts CW.** 2011. SWI/SNF nucleosome remodellers and cancer. Nat Rev Cancer **11:**481-492.

786
787
788
789
790
791
792
793
794
795
796
797
798

799 **Tables and Figure Legends**

800 **Tab 1.** Overview Oligonucleotides.

Primer no.	Primer description	Primer sequence
1371	18S rRNA fw	5′- CGGCTACCACATCCAAGGAA -3′

1372	18S rRNA rev	5′- GCTGGAATTACCGCGGCT -3′
1441	Hexo fw	5′- CGCTGGACATGACTTTTGAG -3′
1442	Hexon rev	5′- GAACGGTGTGCGCAGGTA -3′
1686	E1A fwd	5′- GTG CCC CAT TAA ACC AGT TG -3′
1687	E1A rev	5′- GGC GTT TAC AGC TCA AGT CC -3′
3356	RNF4 fwd	5′-GGTGGAGCAATAAATTCTAGACAAGC-3′
3357	RNF4 rev	5′-CCACCACAGGCTCTAAAGATTCACAAGTGAGG-3′
2978	RNF4 RTR fwd	5′- CAAGCTCAGAAGGCAGCGGCGGAAGCAACCTCC -3′
2979	RNF4 RTR rev	5′- GGAGGTTGCTTCCGCCGCTGCCTTCTGAGCTTG -3′
3070	RNF4 K5R fwd	5′- GCTCCATGAGTACAGGAAAGCGTCGTGG -3′
3071	RNF4 K5R rev	5′- CCACGACGCTTTCCTGTACTCATGGAGC -3′

801

802

803

804 **Fig. 1. HAdV mediated modulation of RNF4 protein during infection.** (A) H1299
805 cells were infected with either wt virus (H5*pg*4100, left panel) or with an E1B-55K
806 null mutant (H5*pm*4149, right panel) at a multiplicity of 50FFU per cell and
807 harvested after indicated time points post infection. Total-cell extracts were prepared
808 with low salt RIPA buffer, separated by SDS-PAGE and subjected to
809 immunoblotting using RNF4 mouse mAb (kindly provided by Takeshi Urano), Daxx

rabbit pAb 07-471 (Upstate), mouse mAb 2A6 (α-E1B-55K), E4orf6 mouse mAb RSA3, HAdV-5 rabbit polyclonal serum L133, Mre11 rabbit pAb pNB 100-142 (Novus Biologicals, Inc.), rabbit mAb α-E2A (α-E2A/DBP) and mAb AC-15 (anti-β-actin) as a loading control. Molecular weights in kDa are indicated on the left, relevant proteins on the right. (B) H1299 cells transfected with 2µg pFlag-RNF4-WT and infected with wt virus (H5*pg*4100) at a multiplicity of 20FFU per cell and fixed with 4% PFA after 48 h post infection. Cells were labeled with anti-Flag mouse mAb M2 (Sigma-Aldrich, Inc.), detected with Alexa488 (α-Flag; green) and mouse mAb 2A6 (α-E1B-55K), detected with Cy3 (α-E1B-55K; red) conjugated secondary antibody. Nuclei are labeled with DAPI (4,6-diamidino-2-phenylindole). Representative α-Flag (green; Bb, Bf), α-E1B-55K (red; Bc, Bg), DAPI (blue; Ba, Be) staining patterns, overlay of the single images (merge; Bd, Bh) and enlarged overlay (merge; Bi) are shown (magnification x 7600). (C) H1299 cells were infected with wt virus (H5*pg*4100, left and right panel) or an E1B-55K null mutant (H5*pm*4149, right panel) at a multiplicity of 50FFU per cell and harvested after indicated time points post infection (left panel) or after 48h (right panel). Cell extracts were fractionated into cytoplasm and insoluble nuclear factions. Equivalent amounts of protein for each fraction were separated by SDS-PAGE and subjected to immunoblotting using the Ab indicated in (A) plus rabbit mAb H3 (α-Histone 3). Molecular weights in kDa are indicated on the left, relevant proteins on the right.

Fig. 2. E1B-55K interaction with RNF4 protein. (A) H1299 cells were cotransfected with 2µg pFlag-RNF4-WT and 2µg pE1B-55K. After 24 and 48h post transfection,

cells were fixed with 4% PFA and labeled with α-Flag mouse mAb M2 (Sigma-Aldrich, Inc.), detected with Alexa488 (α-Flag; green) and mouse mAb 2A6 (α-E1B-55K), detected with Cy3 (α-E1B-55K; red) conjugated secondary antibody. Mock cells are transfected but not infected. Nuclei are labeled with DAPI (4,6-diamidino-2-phenylindole). Representative α-Flag (green; Db. Df, Dj), α-E1B-55K (red; Dc, Dg, Dk), DAPI (blue; Da, De, Di) staining patterns and overlays of the single images (merge; Dd, Dh, Dl) are shown (magnification x 7600). (B) H1299 cells were transfected with an empty vector control or a plasmid encoding E1B-55K and harvested 48h post transfection, or were infected with wt virus (H5*pg*4100) at a multiplicity of 50FFU per cell, harvested 24h post infection and total-cell extracts were prepared. Immunoprecipitation of endogenous RNF4 was performed using RNF4 mouse pAb A01 (Abnova), proteins were separated by SDS-PAGE and subjected to immunoblotting. Input levels of total-cell lysates and coprecipitated proteins were detected using mouse mAb 2A6 (α-E1B-55K), RNF4 mouse pAb A01 (Abnova) and mouse mAb AC-15 (α-β-actin) as a loading control. Note that heavy chains (IgH) are detected at 55 kDa. Molecular weights in kDa are indicated on the left, relevant proteins on the right. (C) H1299 cells were cotransfected with 5µg pFlag-RNF4-WT and 3µg pE1B-55K-wt, 6µg SCS (SUMO-conjugation site K104R mutant) or 1.5µg NES (nuclear-export-signal mutant) and harvested 48h post transfection and total-cell extracts were prepared. Immunoprecipitation of pFlag-RNF4 was performed using α-Flag mouse mAb M2 (Sigma-Aldrich, Inc.), proteins were separated by SDS-PAGE and subjected to immunoblotting. Input levels of total-cell lysates and coprecipitated proteins were detected using the Ab indicated in

(B) Molecular weights in kDa are indicated on the left, relevant proteins on the right.

Fig. 3. E1B-55K binding is mediated by several regions in the RNF4 protein. (A) H1299 cells were cotransfected with 2µg of pE1B-55K and 2µg pFlag-empty, pFlag-RNF4-WT, RTR or K5R. Cells were fixed with 4% PFA after 48h post transfection and labeled with α-Flag mouse mAb M2 (Sigma-Aldrich, Inc.), detected with Alexa488 (α-Flag; green) conjugated secondary antibody. Representative α-Flag (green; Bb, Bf, Bk, Bp), α-E1B-55K (red; Bc, Bg, Bl, Bq), DAPI (blue; Ba, Be, Bj, Bo) staining patterns, overlays of the single images (merge; Bd, Bh, Bm, Br) and 2D intensity histogramms (Bi, Bn, Bs) are shown (n=50 cells). Schematic representation of pFlag-RNF4-WT, the pFlag-RNF4-RTR (3 aa mutation in the putative NLS signal K192021R) and pFlag-RNF4-K5R construct (1 aa mutation in the putative ubiquitinylation site). Mutated regions were marked in red. (B) H1299 cells were cotransfected with 2µg of pE1B-55K and 2µg pFlag-RNF4-SIM, ARM or SIM/ARM. Cells were fixed with 4% PFA after 48h post transfection and labeled at indicated in (A). Representative α-Flag (green; Cb, Cg, Cl), α-E1B-55K (red; Cc, Ch, Cm), DAPI (blue; Ca, Cf, Ck) staining patterns, overlays of the single images (merge; Cd, Ci, Cn) and 2D intensity histogramms (Ce, Cj, Co) are shown (n=50 cells). Schematic representation of the mutated pFlag-RNF4 constructs SIM (deletion of SIM 1-4), ARM (deletion of ARM, position 73-83) and SIM/ARM (deletion of SIM 1-4 and ARM). Mutated regions were marked in red. Colocalization of Flag-RNF4 and E1B-55K was analyzed using coloc2 in Fiji (47) and calculated using Pearson's correlation coefficient (R-Value). (C) H1299 cells were cotransfected with a plasmid encoding

879 E1B-55K and pFlag-RNF4-WT, SIM, ARM, SIM/ARM, K5R, K18R, K5/18R and RTR
880 and harvested 48h post transfection and total-cell extracts were prepared.
881 Immunoprecipitation of pFlag-RNF4 was performed using α-Flag mouse mAb M2
882 (Sigma-Aldrich, Inc.). Proteins were separated by SDS-PAGE and subjected to
883 immunoblotting. Input levels of total-cell lysates and coprecipitated proteins were
884 detected using mouse mAb 2A6 (α-E1B-55K), anti-Flag mouse mAb M2 (Sigma-
885 Aldrich, Inc.), and mouse mAb AC-15 (α-β-actin) as a loading control. Molecular
886 weights in kDa are indicated on the left, relevant proteins on the right.

887

888 **Fig. 4. HAdV infection promotes RNF4/Daxx interaction and Daxx Ubiquitin PTM.**
889 (A) H1299 cells were infected with wt virus (H5*pg*4100) at a multiplicity of 50FFU
890 per cell (left panel) and cotransfected with 2µg of HA-Daxx prior to infection,
891 harvested 16 and 36h post infection and total-cell extracts were prepared.
892 Immunoprecipitation of endogenous RNF4 was performed using RNF4 mouse pAb
893 A01 (Abnova), proteins were separated by SDS-PAGE and subjected to
894 immunoblotting. Input levels of total-cell lysates and coprecipitated proteins were
895 detected using mouse mAb 2A6 (α-E1B-55K), RNF4 mouse pAb A01 (Abnova), Daxx
896 rabbit pAb 07-471 (Upstate) and mouse mAb AC-15 (α-β-actin) as a loading control.
897 Note that light chains (IgG) are detected at 20kDa. Molecular weights in kDa are
898 indicated on the left, relevant proteins on the right.

899 (B) H1299 cells stably were transfected with 5µg of pRNF4-Flag and pE1B-55K. Cells
900 were treated with 25mM NEM and 10µM Mg132 and incubated for additional 4h.
901 28h post transfection, cell pellets were resuspended in 1% SDS lysis buffer and

cleared by centrifugation. Modification of Daxx was analyzed by immunoblotting after SDS-PAGE. Input levels of total-cell lysates and immoprecipitated Daxx were detected using Daxx rabbit pAb 07-471 (Upstate), mAb P4D1 (α-Ubiquitin), RNF4 mouse pAB A01 (Abnova) and mAb 2A6 (α-E1B-55K). Molecular weights in kDa are indicated on the left, relevant proteins on the right.

(C) H1299 cells stably were transfected with 10µg pUbiquitin-His and 5µg each of pDaxx-HA, pRNF4-Flag and either pE1B-55K or pE1B-55K-SCM. Cells were treated with 25mM NEM and total-cell lysates were prepared with guanidinium chloride buffer 28h post transfection, subjected to Ni-NTA purification of Ubiquitin-His conjugated proteins. Proteins were separated by SDS-PAGE and subjected to immunoblotting. Input levels of total-cell lysates and Ni-NTA purified proteins were detected using Daxx rabbit pAb 07-471 (Upstate), mAb 6xHis (α-His), mAb AC-15 (α-β-actin) and mAb 2A6 (α-E1B-55K). Molecular weights in kDa are indicated on the left, relevant proteins on the right.

Fig. 5. RNF4 knock down reduces HAdV viral gene expression and progeny production. (A) H1299 shscrambled and H1299 shRNF4 cells were harvested and total RNA was extracted, reverse transcribed and quantified by RT-PCR analysis using primers specific for RNF4. The data were normalized to 18S rRNA levels. The data is presented as relative RNF4 mRNA levels, compared between H1299 shRNF4 and control cells H1299 shscrambled. (B) Endogenous RNF4 protein levels in H1299 shscrambled and H1299 shRNF4 cells were determined by preparing whole-cell extracts followed by SDS-PAGE and immunoblotting using RNF4 mouse mAb

(kindly provided by Urano) and mouse mAb AC-15 (α-β-actin) as a loading control. Molecular weights in kDa are indicated on the left, relevant proteins on the right. (C) 1x10^5 cells (H1299 shscrambled and H1299 shRNF4) were cultivated and absolute cell numbers were determined after the indicated time points. The mean and standard deviations are presented for three independent experiments. (D) H1299 shscrambled and H1299 shRNF4 cells were infected with wt virus (H5*pg*4100) at a multiplicity of 20FFU per cell. The cells were harvested 16 and 48h post infection, total RNA was extracted, reverse transcribed, and quantified by RT-PCR analysis using primers specific for HAdV-C5 E1A and Hexon. The data were normalized to 18S rRNA levels and the mean and standard deviations are presented for three independent experiments. (E) H1299 shscrambled and H1299 shRNF4 cells were infected with wt virus (H5*pg*4100) at a multiplicity of 50FFU per cell. Viral particles were harvested 48 and 72h post transfection and virus yield was determined by quantitative E2A/DBP immunofluorescence staining on HEK293 cells. The mean and standard deviation are presented for three independent experiments. Values are shown as a ratio shscrambled/shRNF4. (F) H1299 shscrambled and H1299 shRNF4 cells were infected with wt virus (H5*pg*4100) at a multiplicity of 50FFU per cell and harvested after indicated time points post infection. Total-cell extracts were prepared, separated by SDS-PAGE and subjected to immunoblotting using RNF4 mouse mAb (kindly provided by Urano), Daxx rabbit pAb 07-471 (Upstate) and mAb AC-15 (α-β-actin) as a loading control. Daxx and ß-actin blots were used for quantitative analysis and amount comparison for Daxx/ß-actin intensity ratio at 48 and 72h p.i.. HepaRG shDaxx cells were cotransfected with 5µg of Flag-Daxx (lower panel) harvested 24h

post transfection and total-cell extracts were prepared. Proteins were separated by SDS-PAGE and subjected to immunoblotting. Input levels of total-cell lysates were detected using Daxx rabbit pAb 07-471 (Upstate) and mouse mAb AC-15 (α-β-actin) as a loading control. Molecular weights in kDa are indicated on the left, relevant proteins on the right. (G) H1299 shscrambled and H1299 shRNF4 cells cotransfected with 5µg shDaxx construct and 24h later superinfected with wt virus (H5*pg*4100) at a multiplicity of 50FFU per cell. Viral particles were harvested 48h post transfection and virus yield was determined by quantitative E2A/DBP immunofluorescence staining on HEK293 cells. The mean and standard deviation are presented for three independent experiments.

Fig. 6. RNF4 affects establishment of viral replication centers. (A) H1299 cells were infected with wt virus (H5*pg*4100) at a multiplicity of 20FFU per cell and fixed with methanol after 48h post infection. Cells were labeled with α-PML pAb NB 100-59787 (Novus Biologicals, Inc) and rabbit mAb α-E2A/DBP, detected with Alexa488 (α-PML; green) and Cy3 (α-E2A/DBP; red) conjugated secondary antibody. Nuclei are labeled with DAPI (4,6-diamidino-2-phenylindole). Overlay of images (merge; d, j) and corresponding enlarged overlay (merge; e, f) staining patterns are shown. E2A/DBP staining was quantified and analysed by counting the ratio between diffuse and replication center localization in infected cells. (B) Model of crosstalk between RNF4, Daxx and E1B-55K. Schematic representation illustrating a proposed model linking of E1B-55K dependent Daxx restriction and modulation by cellular factor RNF4. Upon HAdV infection, RNF4 is recruited to the nucleus in an E1B-55K-

dependent manner to promote Daxx PTM prior to proteasomal degradation to counteract the cellular chromatin complex and ensure efficient viral gene expression.

Figure 1 Müncheberg et al.

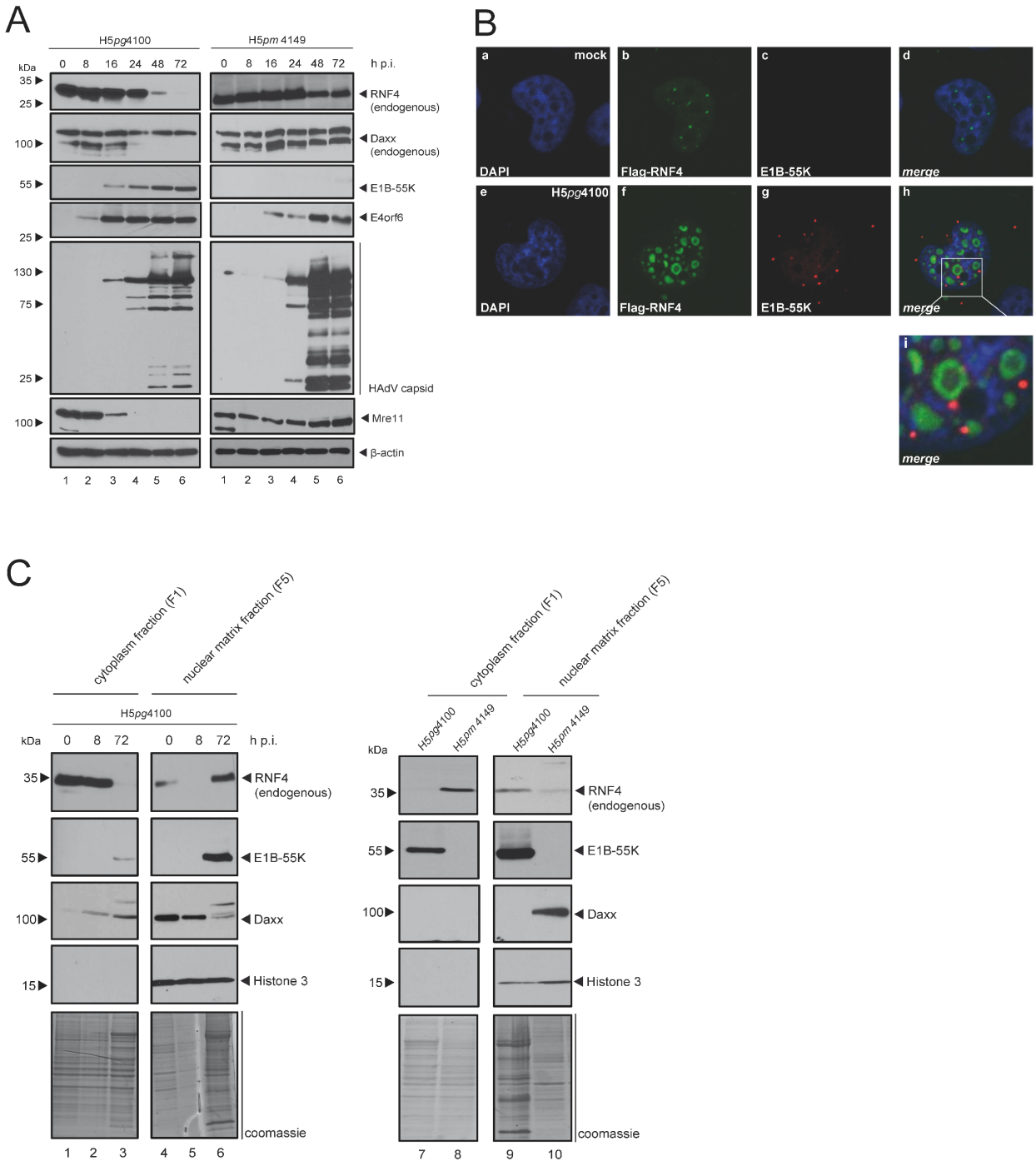

Figure 2 Müncheberg et al.

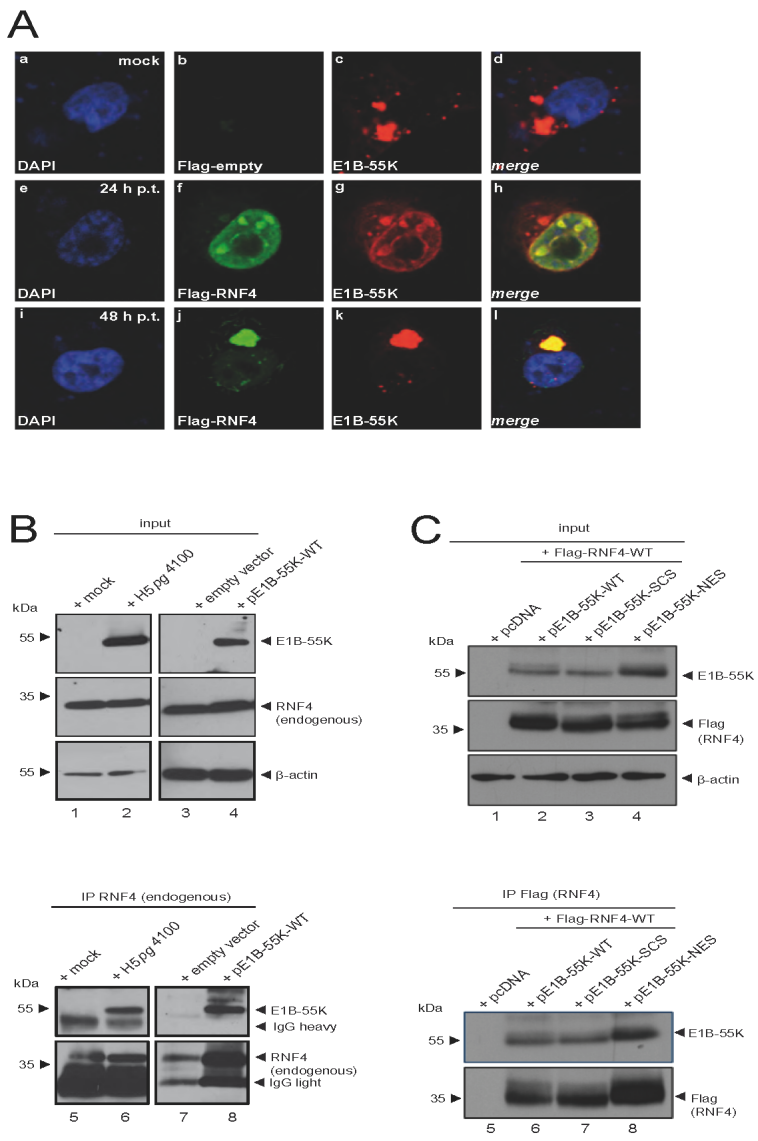

Figure 3 Müncheberg et al.

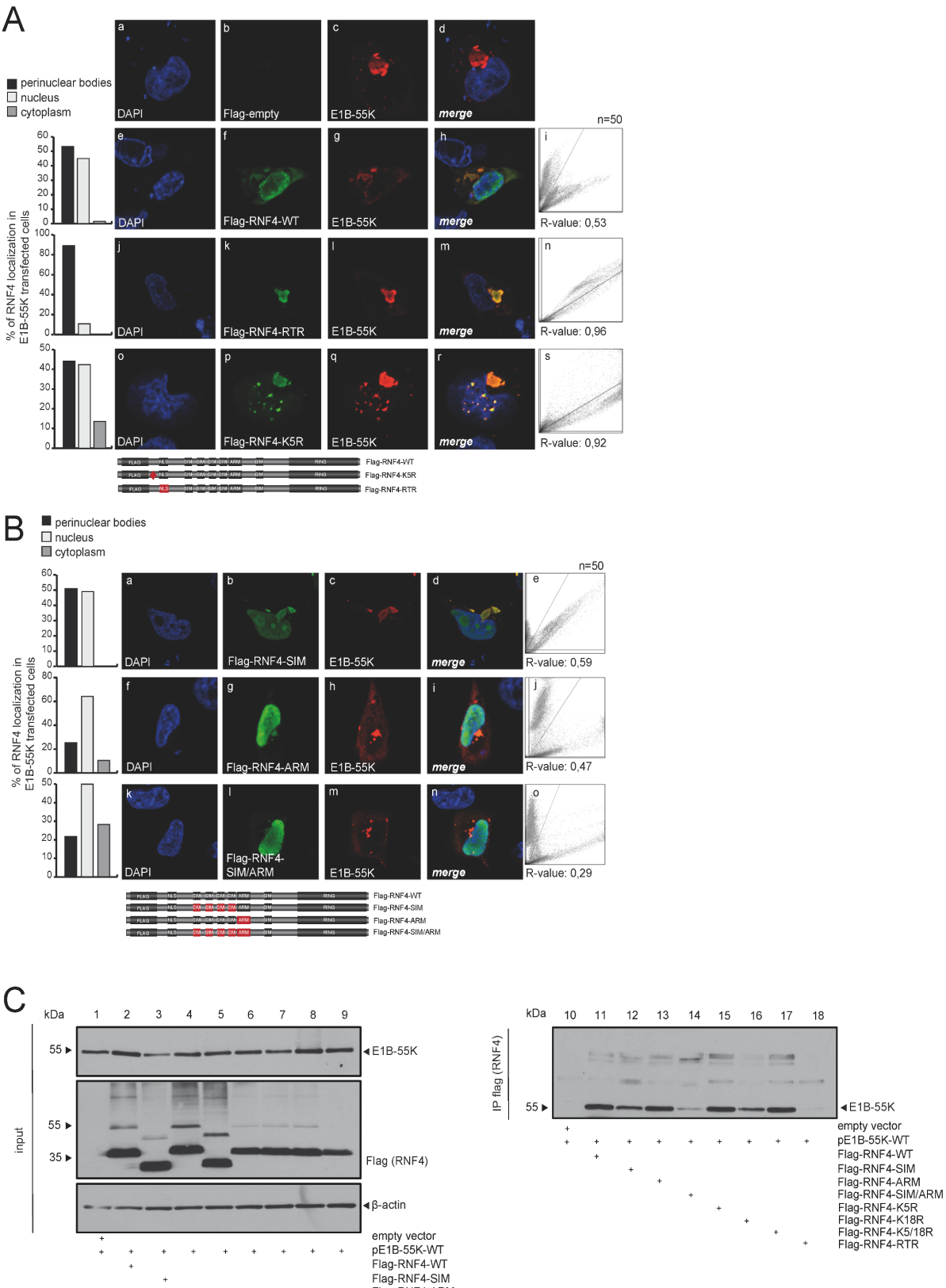

Figure 4 Müncheberg et al

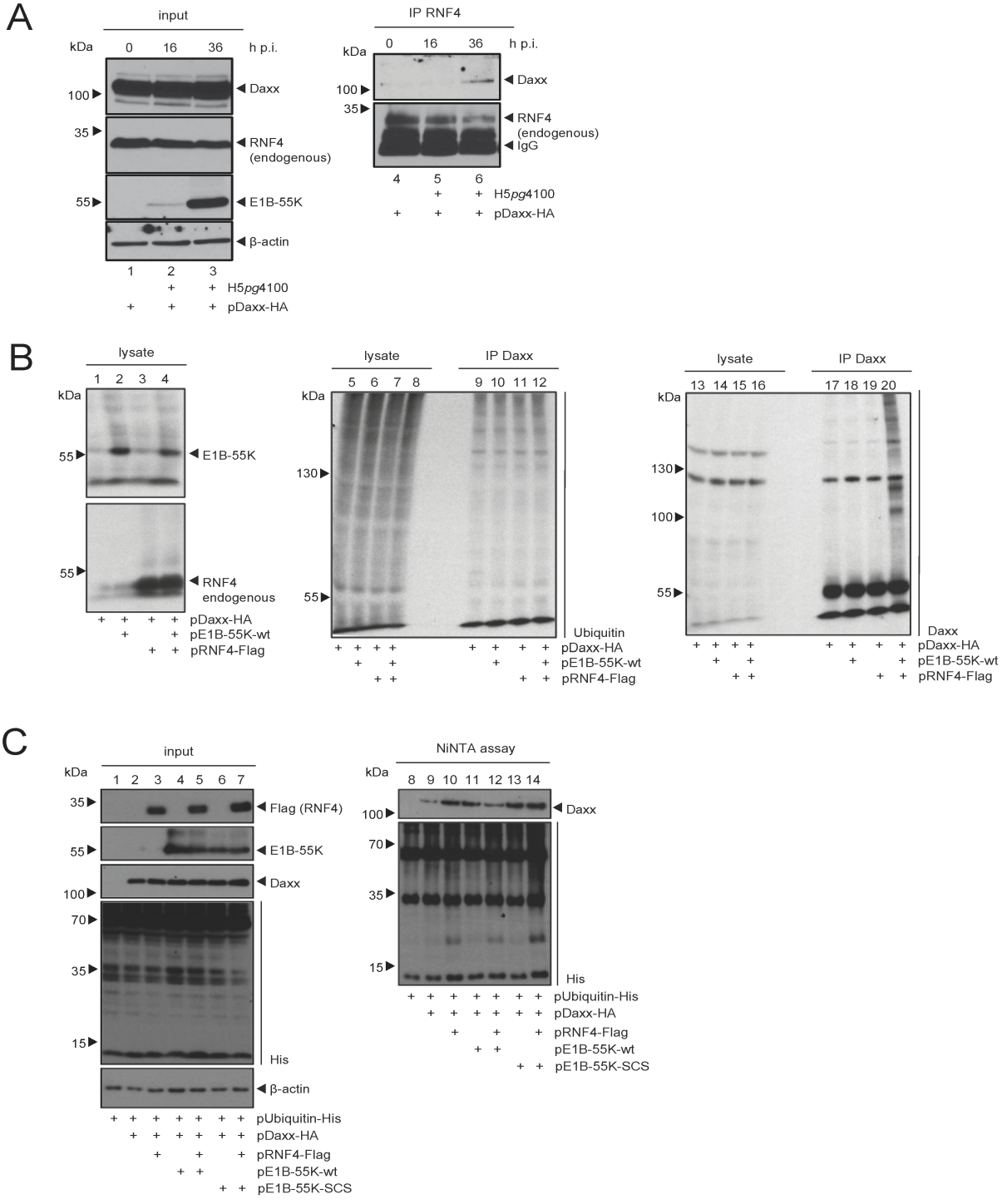

Figure 5 Müncheberg et al.

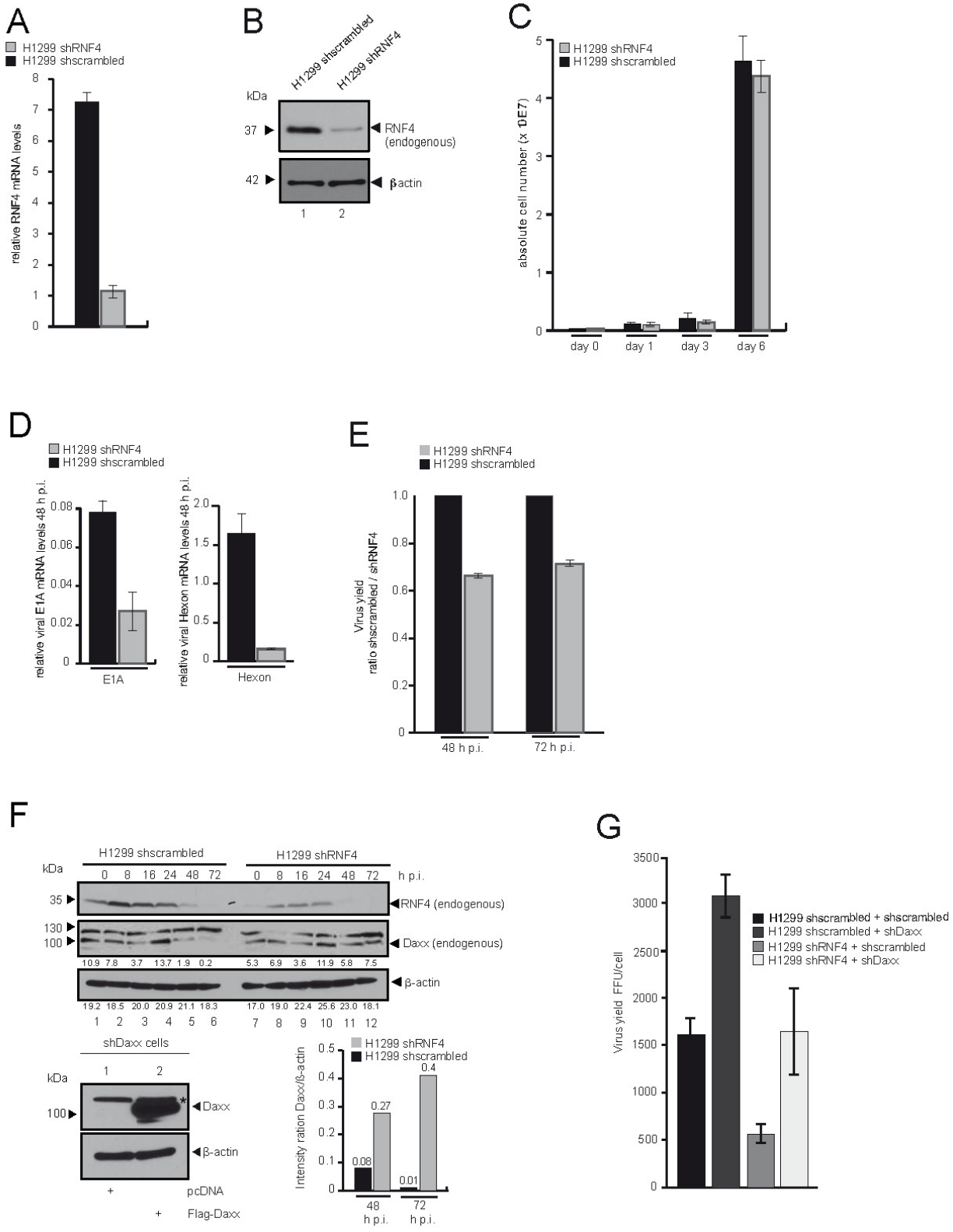

Figure 6 Müncheberg et al.